Ground thermal profile and frost depth in the vicinity of through-grade culverts

Ahmed Moussa, Ahmed Shalaby, Leonnie Kavanagh, Pooneh Maghoul
Department of Civil Engineering, University of Manitoba, Winnipeg, Canada

ABSTRACT

Frost action in soil foundation may adversely affect the pavement structure and the structural integrity of buried utilities such as pipelines and culverts. The seasonal temperature variations, and thermal disruption due to existing buried structures such as culverts are some of the reasons behind the change in the ground thermal profile. The objective of this study was to determine the thermal profile of soil around culverts, and the frost distribution around culverts through a case study of four instrumented culvert sites in *Manitoba, Canada.* The sites varied in the culvert diameter, type of backfill, insulation, and depth of cover. The field thermal data were utilized to calibrate thermal numerical models. The results will provide greater accuracy in predicting the thermal profile and frost distribution around culverts.

RÉSUMÉ

L'action du gel dans le sol de fondation peut défavorablement affectée la structure de la chaussée ainsi que l'intégrité structurale des pipelines et des ponceaux enterrés. Les fluctuations saisonnières de température et l'interruption thermique due aux structures enterrées existantes comme les ponceaux constituent une des raisons expliquant le changement dans le profil thermique du sol. Le but de cette étude était de déterminer le profil thermique du sol et la distribution du gel autour des ponceaux par l'étude de quatre sites instrumentés au Manitoba. Le diamètre des ponceaux, le type et l'épaisseur du remblai, ainsi que l'isolation varient dans chaque site. Les données thermiques in-situ ont été utilisées pour calibrer les modèles numériques thermiques. Les résultats fourniront une meilleure précision dans la prédiction du profile thermique et la distribution du gel autour des ponceaux.

1 INTRODUCTION

Through-grade culverts are required at certain locations to transport water below pavement structure. The performance of roadways over culverts is relatively affected by the deformations in the subgrade, caused by the quality of construction, or differential frost heave, or both (Pierre and Humphrey, 2007; Robson et al 2011; Kavanagh et al, 2017). In general, roadways in cold regions experience distresses resulting from frost action e.g., differential frost heave, and differential settlement during thaw.

The severity of differential frost heave around culvert increases because of the non-uniform compaction of the backfill and the soil-culvert interaction, which limits the soil movement because of the rigidity of concrete culverts (Salem et al, 2008). The frost actions in the soil occur where the soil temperatures drop below the freezing point, continual supply of water, and presence of frost-susceptible soil, all affected by the disruption of the ground thermal profile.

The depth of the active layer, which is the layer where soil experience seasonal freeze and thaw cycles, varies depending on the seasonal climatic variations, and the underground heat or cooling sources e.g., culverts and pipelines. Man-made contribution in the ground disturb the ground thermal regime. Nixon (1978) explained that pavement surface changes the ground thermal profile, which lead to change in the depth of the active layer. Buried culverts affect the ground thermal regime as well as the thickness of the active layer. Therefore, accurate predictions of the ground thermal profile around culverts would provide useful information about thermal profile and frost depth around culverts, which will be useful during the early stage of the geotechnical design of any project.

Four culvert sites were selected along the Provincial Truck Highway 68 (PTH68) in *Manitoba, Canada,* for this study to evaluate the effect of culvert openings on the changes in the ground thermal profile of the road embankment.

2 PROJECT BACKGROUND

The case study consisted of four instrumented culvert sites located along the Provincial Truck Highway 68 (PTH-68), near the town of *Arborg, Manitoba, Canada* (Figure 1).

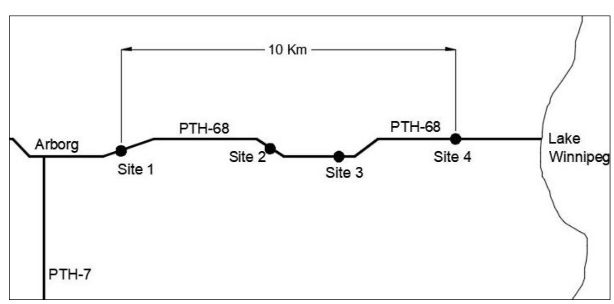

Figure 1. Culvert site locations on PTH-68

Each site consisted of double barrels Portland Cement Concrete (PCC) culverts under 100mm asphalt pavement, and 525mm granular base over granular or clay backfill, all rested on high plastic clay subgrade (A-7-6) (Figure 3). The site investigation report for the sites showed that the average moisture content in the clay subgrade was 25%, with liquid limit, plastic limit and plasticity index of 20%, 50% and 30% respectively. The average densities of the clay backfill and the granular backfill were 1600 kg/m^3 and 1500 kg/m^3 respectively. The sites were different in the type of backfill, culvert diameter, rigid thermal insulation, depth of cover which is measured from the road surface to the top of the culvert barrels (Table 1). Sites 1 and 4 were backfilled with clay soil. Whereas, sites 2 and 3 were backfilled with granular soil. A 50mm thick rigid thermal insulation with thermal resistivity of 0.88 K. m^2/W (5 $ft^2.h.^oF/Btu$) was installed below the culvert at the sites 3 and 4 (Figure 2) to determine their efficiency in reducing the frost penetration depth.

Table 1. Summary of the sites

Site	Backfill	Culvert Outer Diameter (m)	Depth of Cover (m)	Rigid Insulation
1	Clay	1.8	2.8	NO
2	Granular	1.95	1.9	NO
3	Granular	2.01	1.3	YES
4	Clay	1.8	0.8	YES


Figure 2. Rigid insulation placement at site 3

The general layout of the thermistors and insulation, are shown in Figure 3. The depths of thermistors and rigid insulation were measured from road surface shown in Table 2 and illustrated in Figure 3. Each site was instrumented with two sets of thermistors to monitor the ground thermal profile, a U-shaped string with 13 thermistors, and an L-shaped string with 6 thermistors (Figure 3) and (Figure 4). The temperature data was collected on hourly basis using a Campbell scientific data logger installed in each site, and the data download was done annually at each site (Figure 5).

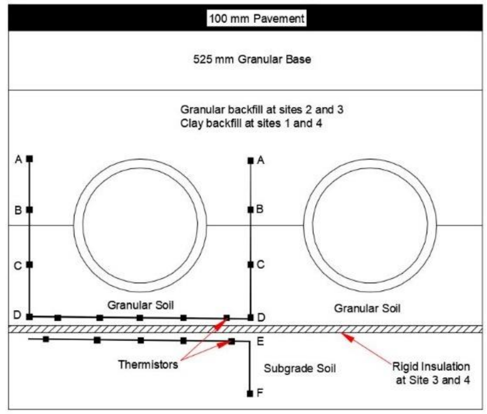

Figure 3. General layout of thermistors in all the sites (Not to Scale)

Table 2. Depth of thermistors in each site in meters

Sites	Depth[1] of Rigid Insulation	Thermistor No.	Depth[1] of Thermistor
Site 1	-[2]	A	2.8
		B	3.4
		C	4.0
		D	4.6
		E	4.7
		F	5.4
Site 2	-	A	2.0
		B	2.6
		C	3.2
		D	3.8
		E	4.0
		F	4.6
Site 3	3.3	A	1.4
		B	2.0
		C	2.6
		D	3.3
		E	3.4
		F	4.0
Site 4	2.7	A	0.8
		B	1.4
		C	2.0
		D	2.6
		E	2.8
		F	3.4

[1] Depths were measured from road surface
[2] No Rigid Insulation installed in the site

a) U-shaped Thermistor String.

b) L-shaped Thermistor String.

Figure 4. Placement of field instrumentation in site 3

Figure 5. On site data download from the Campbell scientific data-logger

3 NUMERICAL MODELING

A 2-D numerical model was developed, using ABAQUS/CAE, to model the ground thermal profile around the culvert (Figure 6), with controlled mesh not to exceed 0.1m width for each of the sites. The total depth of the model was 8 m and the total width was 7 m.

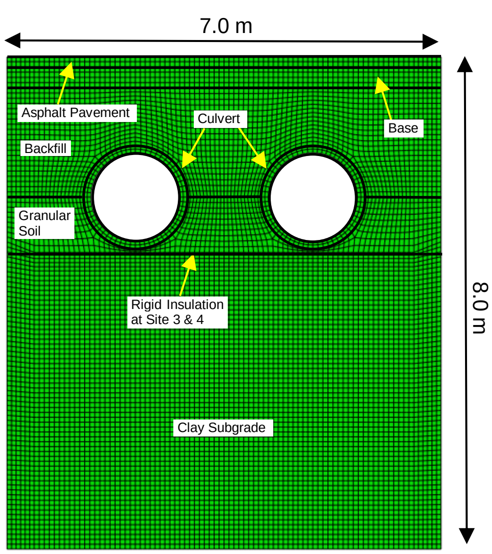

Figure 6. Numerical model geometry and mesh distribution.

The material properties required for the thermal model were thermal conductivity (Eq. 1 to Eq. 4), and specific heat capacity (Eq. 5), which was determined using the volumetric heat capacity of soil (Eq. 6 and Eq. 7). The latent heat (Eq. 10) was required as a separate input to the numerical model, because it would be added to the specific heat capacity during the analysis (ABAQUS manual, 2012). The thermal conductivities and the volumetric heat capacities were determined using the empirical relations developed by Kersten (1949) for clay and granular soil in both frozen and unfrozen states.

- Thermal Conductivity:

Unfrozen Soil:

$$k_{clay} = 0.1442*(0.9*\log(w)-0.2)*10^{0.6243\rho_d} \quad [1]$$

$$k_{granular} = 0.1442*(0.7*\log(w)+0.4)*10^{0.6243\rho_d} \quad [2]$$

Frozen Soil:

$$k_{clay} = 0.001442*10^{0.373\rho} + 0.01226*w*10^{0.4994\rho_d} \quad [3]$$

$$k_{granular} = 0.01096*10^{0.8116\rho} + 0.00461*w*10^{0.9115\rho_d} \quad [4]$$

where k_{clay}, $k_{granular}$ are the thermal conductivities of clay and granular soil respectively in (Watt/m.°C); w is the moisture content; and ρ_d is the dry density of soil in (g/cm^3)

- Specific heat capacity and volumetric heat capacity:

$$c_m = c_v/[\rho(1+w)] \quad [5]$$

$$c_{vu} = (\rho_d/\rho_w)*(0.17+w)*c_{vw} \quad [6]$$

$$c_{vf} = (\rho_d/\rho_w)*(0.17+w_u+0.5w_f)*c_{vw} \quad [7]$$

where c_{vu}, c_{vf} are the heat capacity per unit volume for unfrozen and frozen soil respectively in (MJ/(kg.°C)); ρ, ρ_w are the densities for dry soil and water respectively in (kg/m^3); w is the moisture content; c_{vw} is the volumetric heat capacity of water (4.187 MJ/(m^3.°C)); and c_m is the specific heat of soil in (MJ/(kg.°C)); w_u, w_f are the unfrozen and the frozen water contents in soil determined using Tice et. al. (1976) model as presented in Eq. 8 and Eq. 9

$$w_u = \alpha T^{\beta} \quad [8]$$

$$w_f = w - w_u \quad [9]$$

where w_u is the unfrozen moisture content in frozen soil; w is the soil moisture content; T is the absolute soil temperature below freezing point in (°C); α, β are soil constants depend on the type of the soil, the typical values for α and β were 21.1 and -0.238 respectively for Regina's soil, which assumed to be similar to Manitoba's soil.

- Latent Heat :

$$L = \rho_d*L'*(w-w_u) \quad [10]$$

where L is the volumetric latent heat of fusion in (kJ/m^3); L' is the mass latent heat of water at 0°C which is typically

333.7 kJ/kg; ρ is the dry density of soil (kg/m^3); w, w_u are the total moisture content and the unfrozen moisture content respectively.

The input parameters for the numerical model were determined using Eq. 1 throughout Eq. 10 and are presented in Table 3. The thermal properties of the hot mix asphalt layer presented in Table 3 were based on the values determined by Luca and Mrawira (2005) for asphalt mixture similar to the ones used in the sites.

Table 3. Input parameters for the numerical model

Material properties	Soil Status	Hot mix Asphalt	Granular Base/ Granular Backfill	Clay Sub-grade/ Clay Backfill
Specific Heat (kJ/kg.°C)	Frozen	0.674[1]	1.174	0.995
	Unfrozen	0.674[1]	0.909	1.407
Thermal Conductivity (kJ/hr.m.°C)	Frozen	5.4[1]	0.650	0.886
	Unfrozen	5.4[1]	2.041	3.841
Latent Heat (kJ/kg)	-	N/A[2]	1.299	1.320
Solidous[3] Temp (°C)	-	-	-4	-4
Liquidus[3] Temp (°C)	-	-	0.0	0.0
Dry Density (kg/m^3)	-	2371	1500	1600

[1] based on the work of Luca and Mrawira (2005)
[2] not applicable because moisture content in asphalt layer is negligible
[3] Solidous and liquidus temperatures are the upper and lower temperature limits of phase change range (ABAQUS/CAE manual, 2012)

4 BOUNDARY CONDITIONS

The boundary conditions considered in the model were the surface boundary condition, deep soil boundary conditions, and culvert barrels boundary condition (Figure 7).

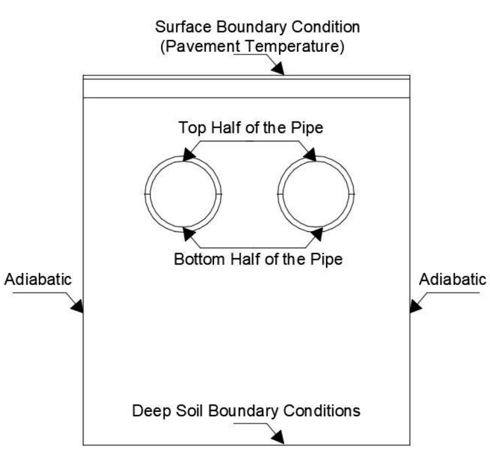

Figure 7. Numerical Model Boundary Conditions

4.1 Surface Boundary Condition

Pavement temperature as the surface boundary condition in thermal models was complex to model. Several models could be used to determine the pavement temperature e.g., the n-factor, the Strategic Highway Research (SHRP) model, the Canadian Strategic Highway Research (C-SHRP) model, and the Long-Term Pavement Performance (LTPP) model. However, the n-factor was recommended, as it had the highest accuracy in determining the ground thermal profile below pavement surface in the statistical testing at 95% level of confidence (Moussa et. al., 2018). The freezing and thawing n-factors for pavement were 0.95 and 1.6 respectively for all the sites.

4.2 Culvert Boundary Condition

The n-factor method was used to determine the concrete culvert temperature from measured air temperature. The factors were determined by back calculating the measured soil temperatures around the culvert barrels. The inner surface of the culvert barrels was divided to an upper and lower half (Figure 7), because the top half was subjected to air most of the year except during spring. While the bottom half of the culvert was covered either by water or ice most of the year, which made it colder than the upper half. The freezing and thawing indices for the upper half were 0.6 and 1.2 respectively. While The freezing and thawing indices for the lower half were 0.95 and 1.6 respectively.

4.3 Deep Soil Boundary Condition

The deep soil boundary condition was located at the depth where ground temperature was independent from the thermal disturbance resulting from pavement structure and the culvert openings. In other words, the deep soil boundary condition was located at the depth where ground temperature was constant all year long. The field instrumentation showed that there was fluctuation in ground temperature as deep as 5.4m, which was the deepest thermistor at the sites. The measured soil temperature was interpolated with depth using Eq. 11 throughout Eq. 14 (Andersland and Ladanyi, 2004; Dore and Zubeck, 2009) and used to determine the depth where ground temperature was steady with time (Figure 8).

$$A_z = A_s*\exp[-z\sqrt{(\pi/\alpha_u*p)}] \quad [11]$$

$$T_{zmax} = T_m+A_z \quad [12]$$

$$T_{zmin} = T_m-A_z \quad [13]$$

$$\alpha_u = k/c_v \quad [14]$$

where A_s is the amplitude of pavement surface temperature (°C); z is the depth measured from pavement surface (m); α_u is the thermal diffusivity (m^2/sec) calculated from Eq. 9; p is the period of time considered in days; A_z is the ground temperature amplitude below pavement surface at depth "z"; T_m is the mean annual temperature of soil at depth "z" which was calculated from filed data; T_{zmax} and T_{zmin} are the maximum and minimum ground temperatures at depth "z"; α_u is the thermal diffusivity in (m^2/sec); k is the soil thermal conductivity in (J/s.m.ºC); and c_v is the volumetric heat capacity in (J/m^3.ºC).

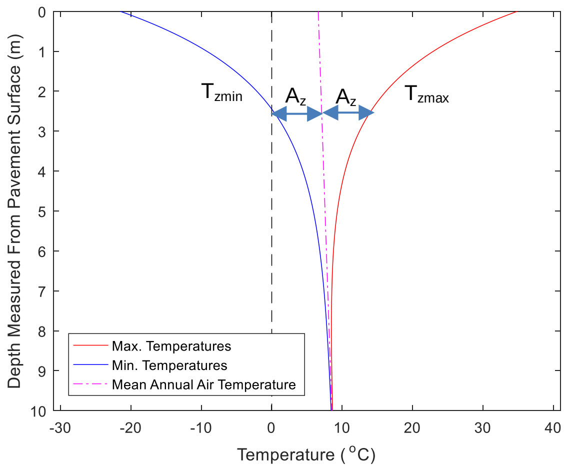

Figure 8. Change in the maximum and the minimum annual ground temperature with depth.

Based on Figure 8 the subsurface boundary conditions were selected at a depth of 8 m where ground temperature was equal to 9.5 ºC, with variation less than 0.3ºC/year. The sides of the model were assumed to be adiabatic, meaning heat transfer was not allowed along the sides of the model.

5 ANALYSIS AND DISCUSSION

Temperature data collected from December 2015 to October 2017 was used to validate the numerical model and analyze the findings from the field data. It should be noted that site 3 was constructed in November 2016. Therefore, the data collected from site 3 was between November 2016 to October 2017.

5.1 Numerical Model Validation

The validation of the model was determined by comparing the predicted and the measured ground temperatures for all sites. The results showed that the numerical model accurately predict the ground temperature at various depths for all the sites, with a coefficient of determination of R^2 = 0.97. Figure (9) shows samples of the comparison between predicted and measured ground temperatures from thermistor C at each site.

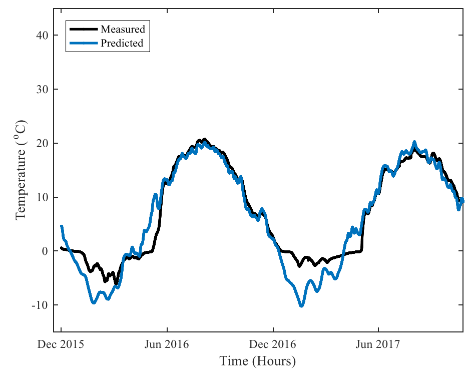

a) Site 1 (Clay Backfill)

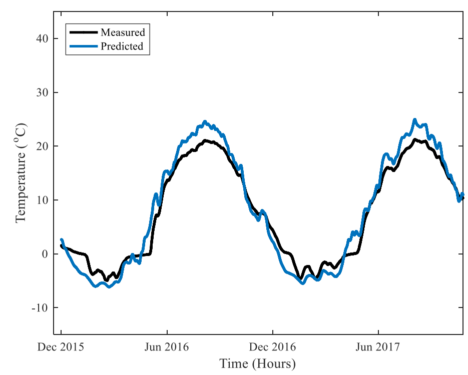

b) Site 2 (Granular Backfill)

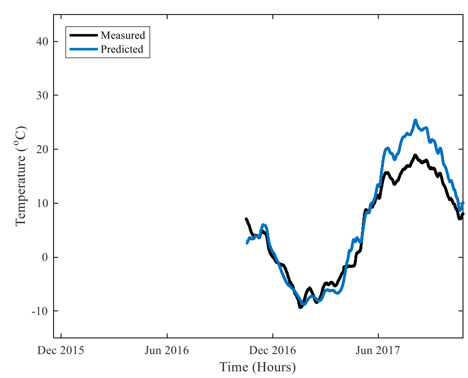

c) Site 3 (Granular backfill)

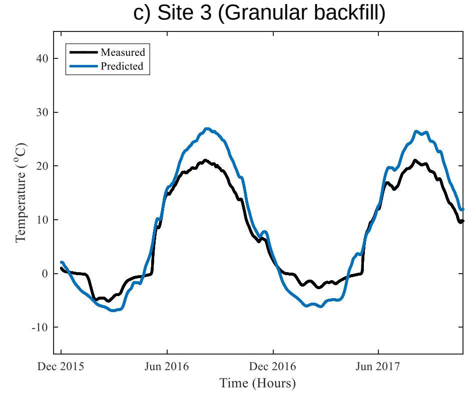

d) Site 4 (Clay backfill)

Figure 9. Predicted and measured ground temperatures from thermistors C.

5.2 Thermal distribution around culverts

The calibrated numerical model was used to predict the thermal profile around the culvert openings for all the sites during several times of the year. Snapshots of the predicted thermal profile at all the sites are shown in Figure 10 throughout Figure 13.

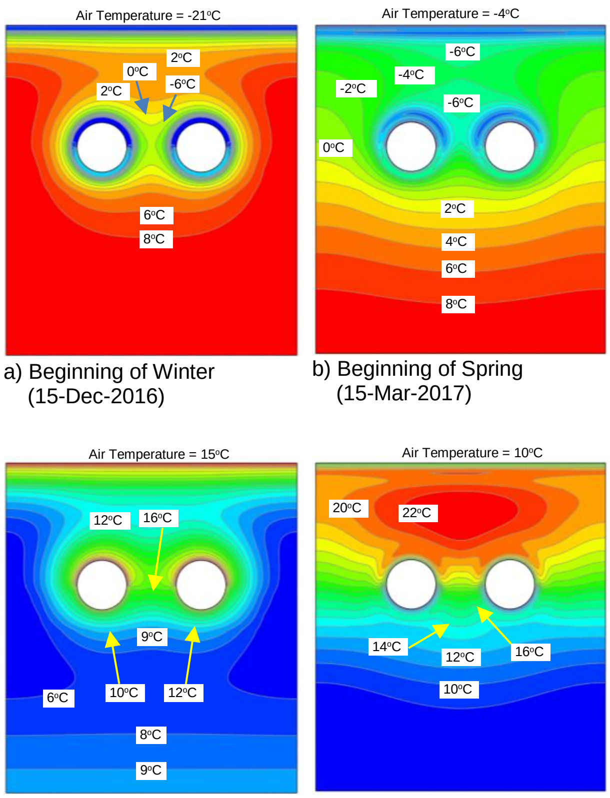

a) Beginning of Winter (15-Dec-2016)
b) Beginning of Spring (15-Mar-2017)
c) Beginning of Summer (15-June-2017)
d) Beginning of Fall (15-Sept-2017)

Figure 10. Thermal distribution around site 1 (Clay backfill).

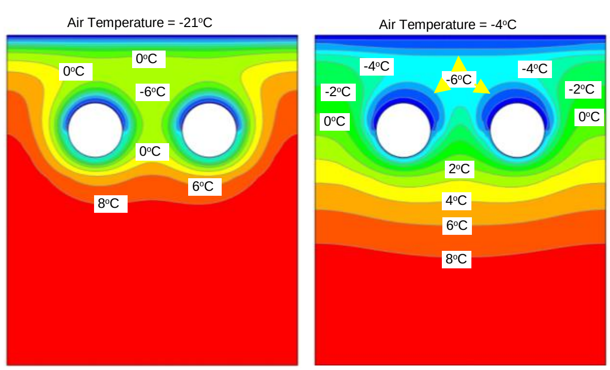

a) Beginning of Winter (15-Dec-2016)
b) Beginning of Spring (15-Mar-2017)

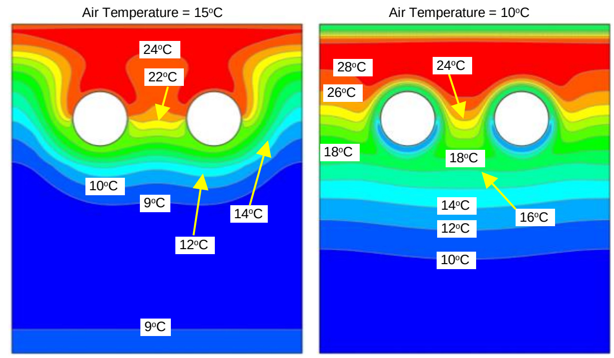

c) Beginning of Summer (15-June-2017)
d) Beginning of Fall (15-Sept-2017)

Figure 11. Thermal distribution around site 2 (Granular backfill).

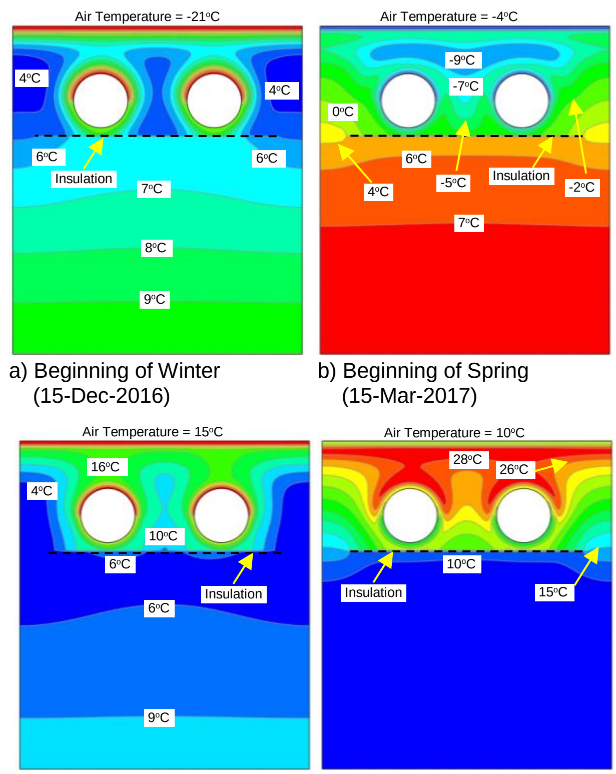

a) Beginning of Winter (15-Dec-2016)
b) Beginning of Spring (15-Mar-2017)
c) Beginning of Summer (15-June-2017)
d) Beginning of Fall (15-Sept-2017)

Figure 12. Thermal distribution around site 3 (Granular backfill + Insulation).

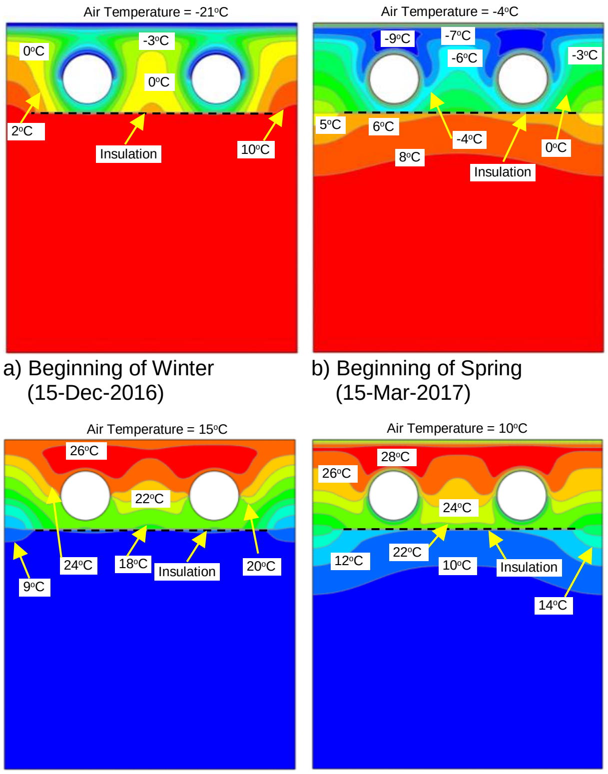

a) Beginning of Winter (15-Dec-2016)

b) Beginning of Spring (15-Mar-2017)

c) Beginning of Summer (15-June-2017)

d) Beginning of Fall (15-Sept-2017)

Figure 13. Thermal distribution around site 4 (Clay backfill + Insulation).

The predicted thermal profiles around the culverts, (Figure (10) throughout Figure (13)), showed that the disruption in the soil thermal profile at the culvert area was caused by the culvert openings. This is because the culverts acted as buried heat source during the Spring and the Summer, and as cooling source during the Fall and the Winter. It was observed that the thickness of the thermally disturbed region around the culvert openings increased as the depth of cover increased. The ground thermal disturbance below the rigid insulation was reduced due to the high thermal resistivity of the insulation (Figure 12 and Figure 13), which kept the ground below the insulation from freezing during the two winters considered in the study.

The freeze and thaw process started from the pavement surface and from the culvert barrels. However, the thermal profile of the ground at sites 2 and 3 were different because of the difference in the backfill materials and thermal properties, and the depth of over.

The culvert openings increased the depth of the active layer, which matched the findings of Nixon (1978). The active layer around the culvert openings was relatively deeper than the depth of the active layer away from the culvert openings (Figure 10-b & Figure 11-b).

5.3 Frost depth around culverts and the effect of thermal insulation

The maximum frost penetration depths and their time of occurrence at each site are shown in Figure 14. The thermally disturbed area (soil that was affected by the culvert) at site 1 was the deepest, because site 1 had the greatest depth of cover, which resulted in having the deepest frost penetration depth (Figure 14-a). The frost penetration did not penetrate through the thermal insulation at sites 3 and 4 as shown in Figures (14-c) and (14-d). This is because the rigid insulation had high thermal resistivity, which prevented disruption in the thermal regime below insulation level.

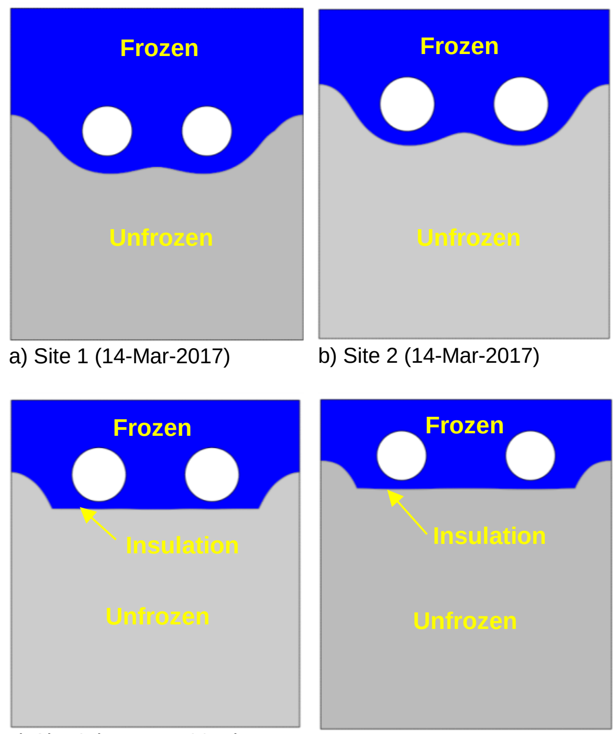

a) Site 1 (14-Mar-2017)

b) Site 2 (14-Mar-2017)

c) Site 3 (14- Mar -2017)

e) Site 4 (14- Mar -2017)

Figure 14. The maximum frost depth without the effect of thermal insulation (a) and (b) and with the effect of thermal insulation (c) and (d).

6 SUMMARY AND CONCLUSION

Four culvert sites were instrumented with two sets of thermistors to monitor the changes in the ground thermal profile around culvert openings and below the pavement surface throughout a period of two years. The sites 1, and 4 were backfilled with clay, while the sites 2, and 3 were backfilled with granular soil. A 50mm thickness of rigid insulation was installed right under the culvert barrels in sites 3 and 4 to examine their efficiency in preventing the soil under the culvert barrels from freezing.

The thermal data collected from the sites were used to calibrate a 2-D numerical model for each of the sites to show the overall thermal regime of the ground around culvert openings throughout a period of two years.

Based on the results, the conclusions from the study are the following:

- The 2D numerical models were able to provide accurate predictions of the ground thermal profile around culverts with R^2 of 0.97.
- The culverts caused disturbance in the ground thermal profile, because they acted as heating source during Spring and Summer, and as cooling source during fall and Winter.
- The thermal disturbance caused by the culverts was the reason behind the increase in the thickness of the active layer around the culvert area.
- The deeper the culvert openings the thicker the active layer.
- The thick layer of frozen soil over culverts were created because of the cooling coming from the culvert openings, which would produce thick layer of weak thawed soil during Spring. This would increase potential roughness at pavement surface.
- The rigid insulation successfully reduced the disturbance in the ground thermal profile, which kept the ground temperature below the insulation above the freezing point.

7 REFERENCES

ABAQUS, C. (2012). Analysis user's manual, Version 6.12.

Andersland, O.B. and Ladanyi, B. 2004. *Frozen Ground Engineering*, 2nd ed., John Wiley and Sons Inc, Hoboken, NJ, USA.

Dore, G. and Zubeck, H.K. 2009. *Cold Regions Pavement Engineering*, 1st ed., McGraw Hill, New York, NY, USA.

Kavanagh, L., Shalaby, A., Moussa, A., Sparrow, S. 2017. Analysis of Measured Strains in Geogrid and Geotextile Reinforcement Clay Backfill Over Through-grade Culverts in Cold Climate, *Transportation Research Board 96th Annual Meeting*, Washington DC, USA.

Kersten, M. 1949. *Laboratory Research for the Determination of the Thermal Properties of Soils*, ACFEL Technical Report 23.

Luca, J., & Mrawira, D. (2005). New measurement of thermal properties of superpave asphalt concrete. *Journal of Materials in Civil Engineering*, *17*(1), 72-79.

Moussa, A., Kavanagh, L., and Shalaby, A. 2018. Evaluating Pavement Surface Temperature Prediction Models in Determining Soil Thermal Profile Below Pavement Surface in Cold Regions, *Transportation Research Board 97th Annual Meeting*, Washington DC, USA.

Nixon, J.F. 1978. Foundation Design approaches in permafrost areas, *Canadian Geotechnical Journal*, 15: 96-112.

Pierre, M., and Humphrey, D. 2007. *Alternative Shallow Cross Pipe Installation Methods*, Main Department of Transportation, Report No. ME 04-1.

Salem, S., Najafi, M. Salman, B., Calderon, D., Patil, R., and Bhattachar, D. 2008. *Use of Trenchless Technologies for a Comprehensive Asset Management of Culverts and Drainage Structures*, University of Wisconsin Department of Civil and Environmental Engineering, Report No. MRUTC 07-15.

Tice, A.R., Anderson D.M., Banin A. 1976. *The prediction of Unfrozen Water Contents in Frozen Soils from Liquid Limit Determinations*, U.S. Army Cold Regions Research and Engineering Laboratory Report CRREL 76-8.